Particle Accelerators
1984 Vol. 14 pp. 155-184
0031-2460/84/1403/0155$18.50/0

COMPENSATED PROTON-BEAM PRODUCTION IN AN ACCELERATING RING AT A CURRENT ABOVE THE SPACE-CHARGE LIMIT

G. I. DIMOV and V. E. CHUPRIYANOV

Institute of Nuclear Physics, 630090, Novosibirsk 90, USSR

(*Received April 26, 1983*)

Results of experiments on the storing of intense proton beams in an accelerating ring by the charge-exchange method are presented. Compensation of the proton space charge allows proton-beam production in the ring with a current one order of magnitude higher than the space-charge limit. Studies have been made of the conditions for stabilization of the beam-beam instability, which is the major obstacle to the production of intense compensated proton beams.

An analysis has also been made of secondary plasma formation in the beam region because of residual gas ionization along the accelerator orbit by fast protons and secondary electrons.

A method has been developed and analyzed for plasma creation in the accelerator through ionization of the residual gas by a flux of electrons traveling along a guiding magnetic field. Proton storage has been studied as a function of plasma density.

INTRODUCTION

At present, the experimental possibilities of high-energy physics are determined mostly by the state of development of particle accelerators. One of the major problems in acceleration technique is to increase the intensity of charged-particle beams.

For the past 15–20 years, much progress has been achieved in the increase of intensity of the beams produced in ring accelerators. The main instabilities of the beams of charged particles in accelerators and storage rings have been investigated. Effective methods of suppressing coherent oscillations of accelerated particles have been developed. The method of charge-exchange proton injection, developed at the Novosibirsk Institute of Nuclear Physics,[1–4] is being used more and more intensively. This method enables the phase density of the accelerator beam to increase considerably compared with the phase density of particles in the injected beam. High-current sources of positive and negative ions have also been designed. In this connection, defocusing of accelerated particles by the internal electromagnetic fields becomes the main factor that limits the beam intensity in cyclic accelerators.

The space-charge effects of accelerated particles are diverse, but the most serious limitation on the beam intensity is imposed by the incoherent shift of betatron-oscillation frequencies. The only way of increasing the number of particles accelerated during one run is to increase the injection energy. Realization of this methods results, as a rule, in construction of an intermediate ring accelerator—the booster. Most large accelerating facilities are equipped with such ring injectors. However, for boosters the intensity problem is of even greater significance. The designers have to complicate substantially the devices (a larger number of accelerating paths, repeated injection) and

to increase their sizes because of the limitation on the number of accelerated particles per cycle.

As was at first pointed out by G. I. Budker,[5] in induction ring accelerators of positive ions there is a possibility in principle of unlimited increase of the number of accelerated particles by the compensation of their space charge by electrons. Such compensation eliminates the restriction on the beam intensity associated with the shift in the betatron frequencies of incoherent oscillations of protons. The beam instability connected with the shift of coherent frequencies lies much higher in intensity, and can in principle be suppressed, for example, by feedback systems.

It seems to be possible to perform induction acceleration of such a compensated beam up to an energy of 500 to 1000 MeV. At this energy, a compact betatron with intensity unlimited by space charge could compete successfully with the operating boosters of proton acceleration facilities and with those being constructed. These medium-energy intense proton beams can be extensively utilized in neutron physics for the production of powerful neutron pulses. The possibility is not excluded of creating high-energy induction accelerators according to the scheme of repeated utilization of magnetic flux, which was first proposed by N. Christofilos.[6]

At the Novosibirsk Institute of Nuclear Physics, studies have been made of the compensation of the space charge of a proton beam with electrons. The latter are produced through ionization of the residual gas by circulating protons. In the course of the first experiments at a weak-focusing accelerator with momentum-compaction factor $\alpha > 1$, it has been shown that even a small longitudinal modulation of the proton density leads to the extraction of electrons from the beam region because of their instability.[7] Therefore, in accelerators where the space charge of positive ions is to be compensated by electrons, the momentum compaction factor should be less than unity ($\partial\omega/\partial E > 0$, where ω and E are the revolution frequency and energy of the accelerated particles). Otherwise, the longitudinal instability associated with the "negative-mass" effect[8,9] results in practice in the total decompensation of the beam.

However, the instability of proton motion in a compensation medium is a major problem in intense compensated proton-beam production. A theoretical investigation of the interaction between the circulating beam and the shear from the compensating particles has been made in Refs. 10–12. As has been shown, the transverse "snake" instability should develop in such a system. This instability was experimentally discovered at the INP[7,13–15] and somewhat later at CERN[16,18] and Berkeley.[17] It is this instability that turns out to be the main obstacle to increasing the current in a compensated proton beams.

1. DESCRIPTION OF THE EXPERIMENTAL DEVICE

The experiments that deal with the possibility of storing an intense compensated proton beam have been carried out at a cyclic weak-focusing storage ring of the "racetrack" type (see Fig. 1). This storage ring has four straight sections whose length is larger by a factor of 2.5 than the radius of curvature in the bending magnets. The ratio of the length of the straight and curved sections of the beam orbit has been chosen such that the momentum-compaction factor is less than unity. In comparison with a strong-focusing magnetic system, in which the condition for stability relative to the longitudinal bunching because of the "negative mass" effect mentioned in the Introduction is also satisfied, the scheme chosen is much simpler from a technological point of veiw and the availability of long straight sections allows a large number of control and monitor devices to be placed.

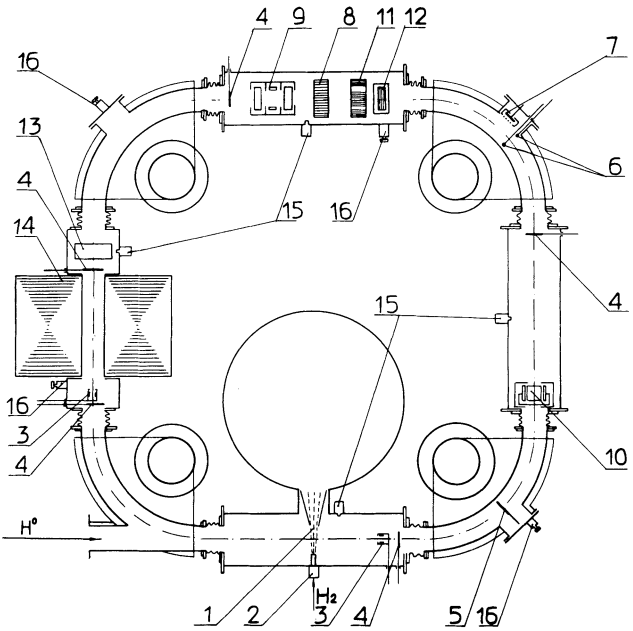

FIGURE 1 Layout of the proton storage ring. 1—secondary stripping gas target, 2—pulsed gas valve, 3—Faraday cups, 4—quartz screens, 5, 6—mobile targets, 7—ion collector, 8—Rogovsky coil, 9—"pick-up" station, 10—electrostatic transducer of quadrupole beam oscillations, 11—magneto-inductance transducer, 12—transducer of vertical beam losses with high time resolution, 13—device for measuring the secondary charged-particle concentration in the beam region, 14—betatron core, 15—electromagnetic gas valves of the system of pulsed gas leak-in, 16—microleaks of the system of stationary gas leak-in.

The main parameters of the storage ring are listed in Table I.

Injection of protons into the storage ring was performed by the charge-exchange method.

The storage-ring magnetic system consists of four identical permanent C-shaped electromagnets with an index of field decrease $n = 0.5$ and four straight sections of equal length. In order to vary the index of field decrease within a broad region, plane correcting bars were mounted between the vacuum chamber and the magnet poles.

For the proton-storage experiments, the range of values of betatron frequencies was chosen to be maximally away from the most dangerous resonances. The correction

TABLE I

Storage-Ring Parameters

1. Proton energy	1 MeV
2. Field intensity in bending magnets	3500 G
3. Index of field decrease	0.2 to 0.7
4. Radius of rotation in magnets	42 cm
5. Length of the straight sections of an orbit	106 cm
6. Aperture of vacuum chambers in bending magnets	6 × 4 cm
7. Revolution frequency of protons in the storage ring	1.86 MHz
8. Duration of injection pulse	up to 300 μsec
9. Repetition frequency of injection pulse	0.2; 0.1 Hz
10. Injection current	up to 8 mA

TABLE II

Betatron-Oscillation Frequencies

Radius (mm)	405	420	435
ν_x	1.66	1.62	1.60
ν_z	0.82	0.84	0.85

current varied within the range 250 ± 30 A. The values of betatron oscillation frequencies on various radii, which have been measured on the circulating beam at a correction current of 250 A, are listed in Table II (see also Fig. 2).

The momentum-compaction factor was equal to 0.5. The calculated trajectory of motion of the operating point versus the number of the protons stored is drawn in Fig. 2. The calculation has been made with the assumption of a beam of elliptic cross section that is homogeneous in azimuth and cross section. The energy losses of the circulating beams, caused by its interaction with gas and in the charge-exchange target, were compensated by an azimuthal electric field in the accelerating gap induced by the magnetic flux from the core. The core winding was excited with a lamp modulator. Due to magnetization reversal between operating pulses, the magnetic induction in it could be changed up to 25 kG. This made it possible to achieve in the gap, an accelerating voltage as high as 350 V with a pulse duration of 500 mc sec.

In order to remove from the circulating beam region the secondary charged particles produced through ionization of residual gas by fast protons, clearing electrodes were

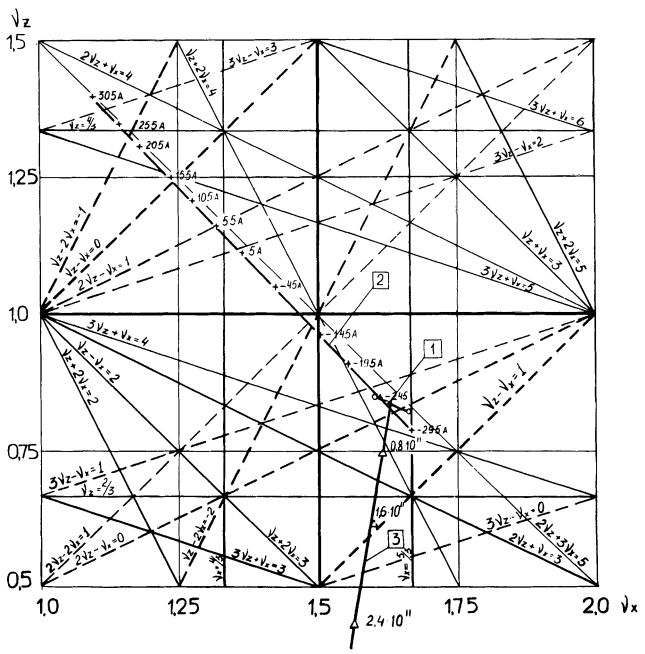

FIGURE 2 Tune diagram of the betatron frequencies of the storage ring. 1—operating values of betatron frequencies measured on the low-intensity beam, 2—calculated trajectory of the operating point while varying the current in the correcting bars; 3—calculated trajectory of the operating point under the action of the space charge forces.

installed throughout the beam orbit in the storage ring. This system of electrodes was a series of plane metallic plates located below and above the circulating beam. The dc voltage supplied to these plates was up to 2 kV. These plates could be all switched off simultaneously in approximately 1 msec. The geometry of the electrodes and alternation of voltage polarity were chosen such that the extracting electric field has negligibly weak influence on the circulating beam.

The parameters of the proton beam in the storage ring were measured with transducers and probes of various kinds. Their arrangement is shown in Fig. 1.

At the proton-beam collection conditions that we are interested in, the density of secondary charged particles, positive ions and electrons produced as a result of ionization of the residual gas, can much exceed the density of protons in the beam. In view of this, in the studies of coherent beam oscillations not only the system of electrostatic electrodes (9, 10 in Fig. 1) with a bandwidth up to 200 MHz, but also a system based on a magneto-inductance transducer (11) with 1–150 MHz bandwidth are both used.

In order to study the dependence of the behavior of the beam-beam instability on the kind of gas, its pressure and distribution around the ring, the storage ring was equipped with two systems for gas leak-in. A stationary leak system consisted of four microleaks (16) and made it possible to fill fairly uniformly the vacuum chambers of the storage ring with various gases over a broad range of pressures. A pulsed system with four electromagnetic gas valves (15 in Fig. 1) permitted the density distribution of gas to be widely varied in azimuth.

The density of secondary ions plays a significant role in the development and stabilization of the transverse beam-beam instability of a proton beam. It was measured with a device (13) whose mode of operation is based on the measurement of the current of charged particles extracted from the beam region by a short (100 nsec) high-voltage (15 kV) pulse.

2. EXPERIMENTAL STUDY OF COMPENSATED BEAM STORAGE

In the first stage of proton-beam experiments, we have analyzed the possibility of stable compensation of the space charge of a proton beam by the electrons produced during ionization of various gases on the orbit by circulating protons.[13–15,19,20]

If the residual gas pressure in the storage ring is minimum and the secondary charged particles are removed from the beam region by an electric clearing field of about 200 V/cm, the beam is stable relative to coherent oscillations. The largest number (about $1.9 \cdot 10^{11}$) of protons stored in these conditions is independent of the injection current over a broad interval and corresponds, according to calculations, to a shift of the incoherent vertical betatron-oscillation frequency of protons by an internal electric field to the linear resonances of $\nu_z = 0.5$. The beam potential measured over the energy spectrum of secondary ions is about 200 V. The measured density of secondary electrons in the beam does not exceed a few percent of the proton density. Beam losses are due to an increase of vertical size up to the storage ring aperture, and are incoherent in nature.

If the clearing voltage is switched off, the concentration of secondary electrons in the beam increases and intense coherent vertical oscillations develop as a result. This is followed by an increase of beam loss in the vertical direction and by a substantial reduction of the current of circulating protons. The lifetime of the protons in the storage ring is decreased by more than a factor of two.[15]

Regularities in the development of transverse oscillations allow us to conclude that their appearance is caused by the development of the beam-beam instability associated with interaction of the proton beam with secondary charged particles produced by ionization of the residual gas.[7]

In order to elucidate the role of the coherent oscillations of the circulating beam in the mechanism of proton loss, the loss in the vertical direction has been observed with a probe of high time resolution. The main part of the loss of circulating protons has been shown to be of coherent nature. The incoherent losses are no higher than 10%.[15]

The spectrum of the signal of proton losses in the vertical direction is similar to that of the beam center of gravity coming from a vertical-position pickup. The latter consists of a large number of narrow bands with centers distributed according to $(k\text{-}\nu_z)f_0$, with k a positive integer. The particular shape of the spectrum depends on the number of stored protons, N_p. At $N_p = 1.5 \cdot 10^{11}$, the spectrum maximum lies in the interval 32 to 46 MHz (k = 16 to 24) and at $N_p = 1.7 \cdot 10^{10}$ in the band 15 to 24 MHz (k = 7 to 12).[14]

An investigation was specially made of the influence of Landau damping on stabilization of the instability under observation. The energy spread of protons in the circulating beam was controlled by varying the magnitude of an azimuthal electric field in the accelerating gap. The Landau damping has a stabilizing influence on the beam-beam instability throughout the accessible range of variation of the spread of proton frequencies. This increases the threshold densities of circulating protons and secondary ions[15] to the development of the instability. However, the influence of Landau damping is limited to this effect and does not alter substantially the general picture of the development of the instability.

At the first stage, the behavior of the proton beam does not qualitatively vary as the gas density in the storage ring increases (see Fig. 3). With an increase in the rate of secondary ion formation (which at the beginning of the collection process is mainly determined by the current of protons and by the density of gas molecules), the instability becomes stronger. This leads to a decrease of the threshold current of oscillations, to an increase of the relative amplitude of oscillations, and to a decrease of the number of stored protons. The density of secondary ions is close to that of protons in the beam and grows slightly as the gas density increases. The maximum of the spectrum for beam oscillations shifts toward higher frequency. However, when a certain gas density is reached, the picture drastically changes (see Fig. 3). After developing up to considerable amplitude at the beginning of storing, the beam oscillations then damp very fast. The proton beam intensity in the orbit increases considerably going beyond the space-charge limit. The course of such a store is illustrated by the solid curves in Fig. 4. For each gas utilized in the experiment, there is a proper threshold over density above which the oscillations damp rapidly. The measured threshold pressures and densities for a number of gases are listed in Table III. The threshold pressure on the track decreases as molecular weight and the ionization cross sections increase and is independent of the injection current (to 8 mA).

A small decrease in the gas pressure relative to the threshold pressure results in oscillations that do not damp and the number of protons stored on the track does not exceed approximately 10^{11}, as the dotted curves indicate in Fig. 4.

A characteristic feature of the process at above-threshold pressures is the collection of secondary ions (and hence electrons) in the circulating beam to high density, higher by one order of magnitude than the proton density. The density of secondary electrons (ions) at above-threshold pressures coincides with the proton density, when the instability begins stabilizing, for most of the tested gases with a high accuracy, and lies in the range 3 to 4 10^8 cm^{-3} (see Fig. 5 at the instant between

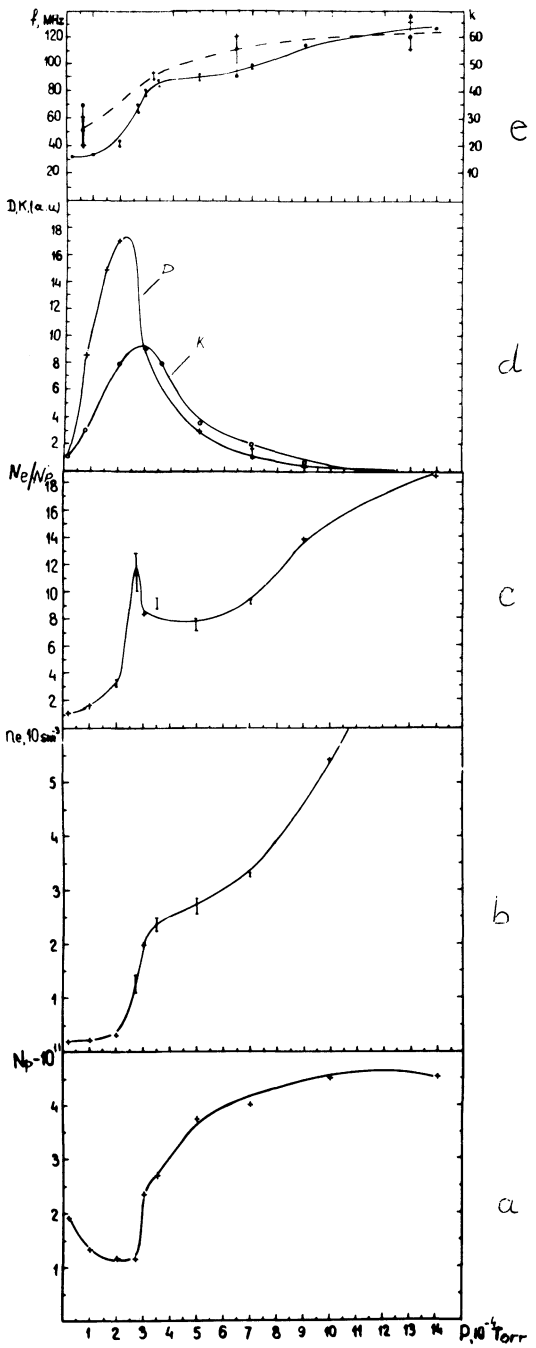

FIGURE 3 The dependences on nitrogen pressure in the storage ring: a—the number of stored protons N_p; b—the mean density of electrons in the beam region; c—ratio of the number of electrons stored in the beam to the number of protons; d—envelopes of rf signals coming from a magneto-inductance transducer when measuring dipole—D and quadrupole—K oscillations; e—the position of a maximum of the spectrum of rf signal from the magneto-inductance transducer when measuring dipole (—) and quadrupole (— — — —) oscillations.

TABLE III
Threshold pressures and densities

Gas	H_2	D_2	H_e	N_2	Ar
Threshold pressure, Torr	$2.6 \cdot 10^{-3}$	$1.7 \cdot 10^{-3}$	$5 \cdot 10^{-3}$	$3.2 \cdot 10^{-4}$	$2.2 \cdot 10^{-4}$
Threshold density, cm^{-3}	$9.2 \cdot 10^{13}$	$6.0 \cdot 10^{13}$	$17.7 \cdot 10^{13}$	$1.1 \cdot 10^{13}$	$7.8 \cdot 10^{12}$

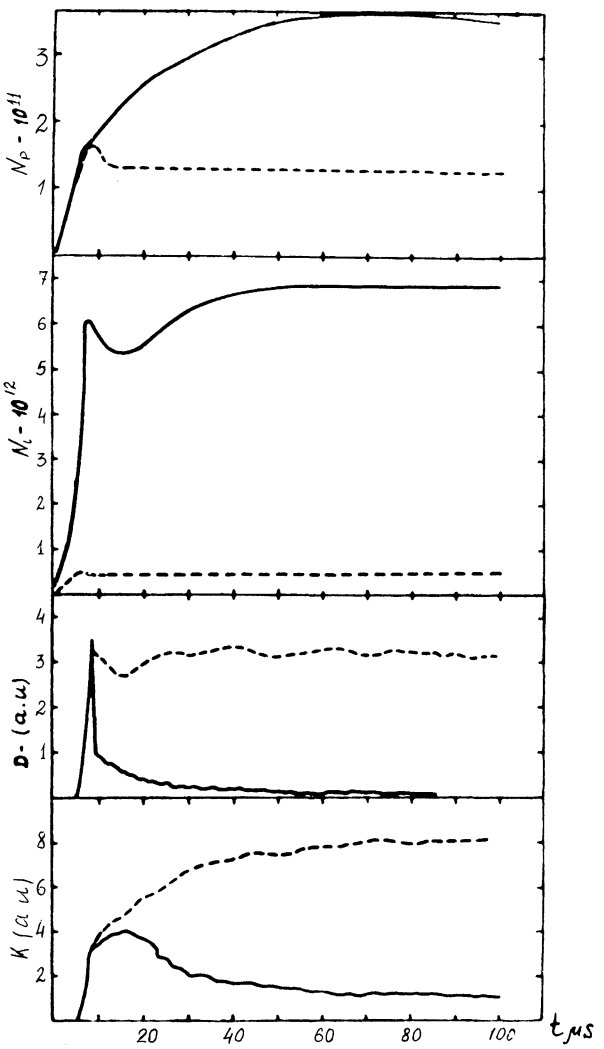

FIGURE 4 The process of proton collection in the compensated beam with hydrogen pressures of $1.4 \cdot 10^{-3}$ Torr (dotted curves) and $3.6 \cdot 10^{-3}$ Torr (solid curves). The current of proton injection is 5.5 mA (when the first turn is completed). N_p is the number of protons in the beam; N_i is the number of secondary ions in the beam; D is the amplitude of rf signals from electrostatic vertical-position electrodes per unit orbital proton current; K is the same for quadrupole electrodes.

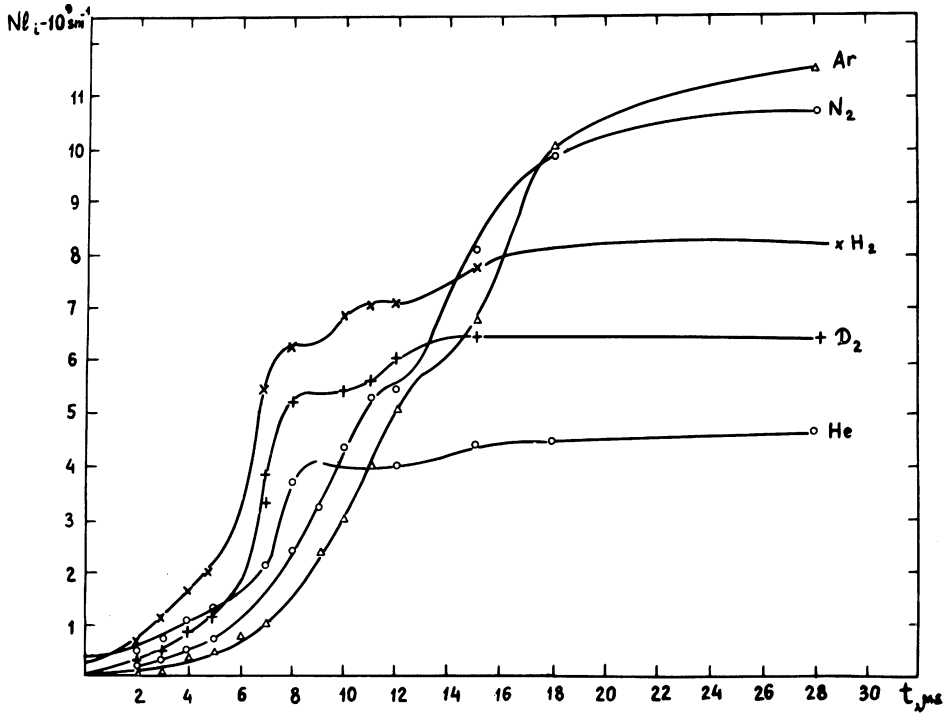

FIGURE 5 Time dependence on linear density of secondary ions at after-threshold pressures on different gases.

10 and 15 microseconds from the beginning of storing). Only the density of helium ions is somewhat lower in this region. The secondary ions are mainly collected in a short period of time whose commencement coincides with the beginning of the development of the transverse instability. The oscillations have no time to build up to an amplitude such that the beam is decompensated or its current is limited. Nevertheless, these decrease the rate of collection of the orbital current.

A small loss of gas pressure, relative to the threshold, leads to a drastic decrease of the ion density and to the development of intense undamped rf oscillations (see Figs. 3 and 4). The time behavior of the ratios between the densities of secondary ions and protons for the cases of light (a) and heavy (b) gases at different pressures are presented in Fig. 6. At above-threshold gas pressures, the relative number of secondary ions in the beam sharply increases in the instability region. In the below-threshold region of pressures, this effect is not observed at all, or is very weak.

To elucidate the dynamics of storing secondary ions in the proton beam, measurements have been made of the time behavior of their density during the accumulation of the proton current. The time dependence of the quantity $N_i/(n_0 N_p v_p)$, where N_i and N_p are the number of stored ions and protons, respectively, n_0 is the gas density on the orbit and v_p is the proton velocity, after the beginning of injection at different pressures of nitrogen is plotted in Fig. 7. The derivative of these curves is equal to an effective "collection cross section" of secondary nitrogen ions normalized to the beam protons, that is, to the difference between the ion production cross section and value of $N_i/(\tau_i n_0 N_p v_p)$, where τ_i is the lifetime of an ion. Note that this value plays

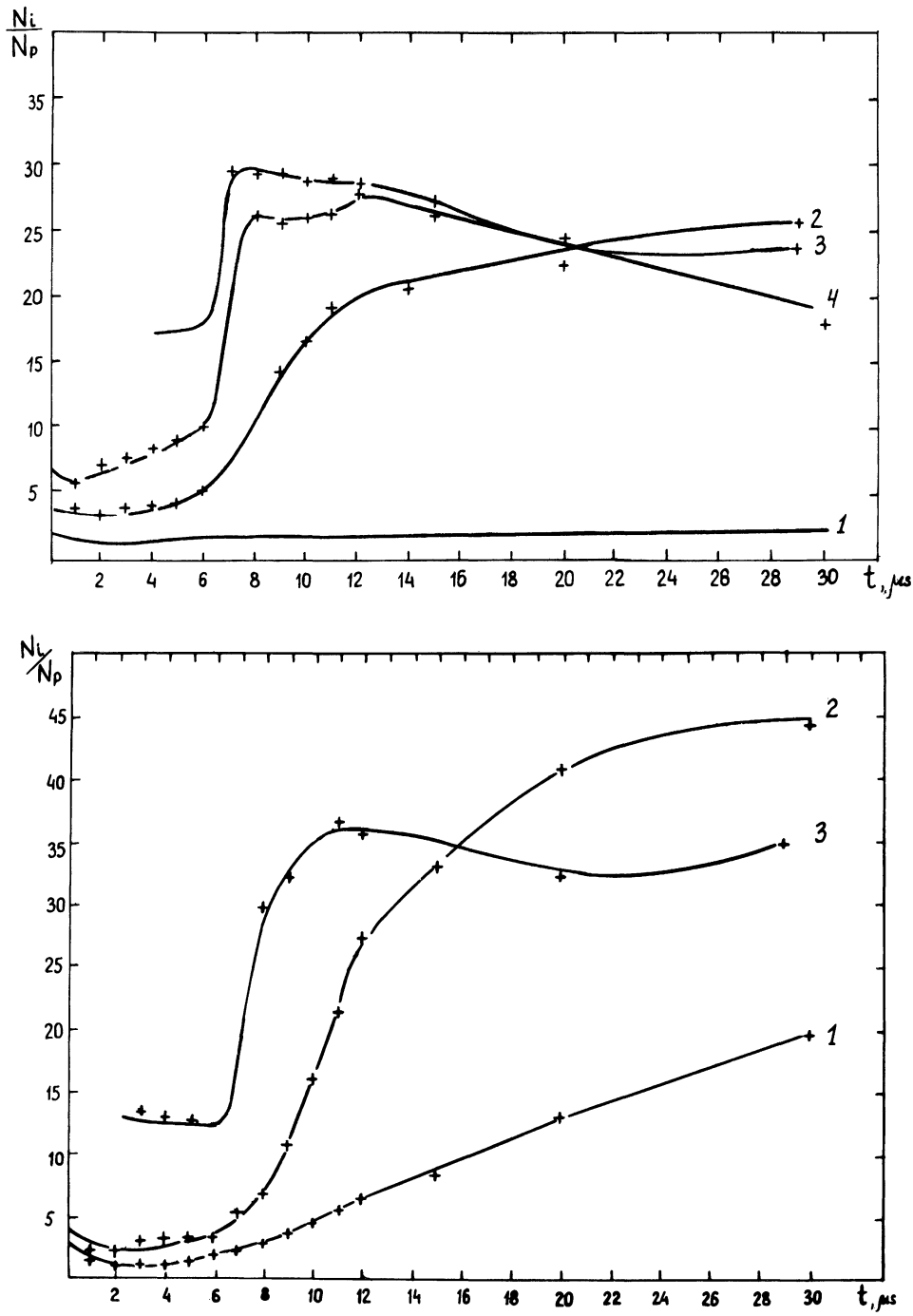

FIGURE 6 Time behavior of the ratio of the number of stored ions in the beam to the number of protons at different pressures: (a) deuterium filled; 1—$P = 4.5 \cdot 10^{-4}$ Torr, 2—$P = 1.1 \cdot 10^{-3}$ Torr (below threshold), 3—$P = 1.7 \cdot 10^{-3}$ Torr (above threshold), 4—$P = 3.6 \cdot 10^{-3}$ Torr; (b) argon is filled: 1—$P = 1 \cdot 10^{-4}$ Torr, 2—$P = 2 \cdot 10^{-4}$ Torr (below threshold), 3—$P = 8 \cdot 10^{-4}$ Torr (above threshold).

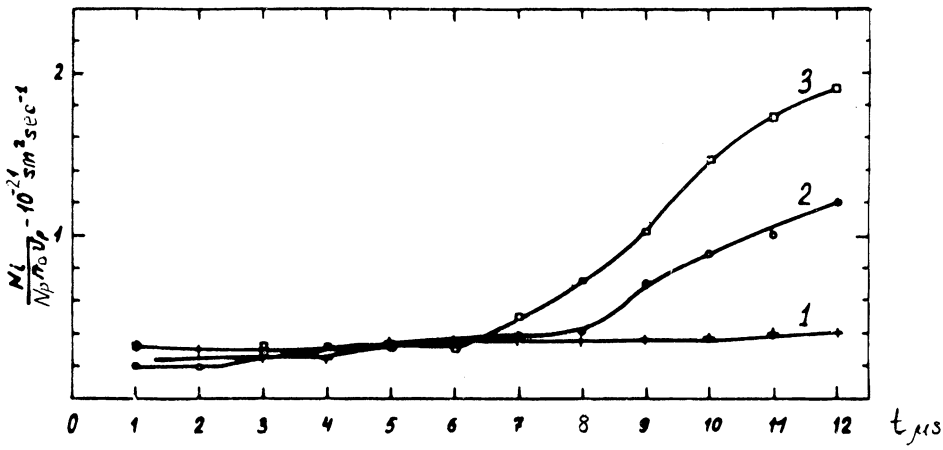

FIGURE 7 1. $\bar{P} = 10^{-4}$ Torr; 2. $\bar{P} = 2.10^{-4}$ Torr; 3. $\bar{P} = 3.6 \cdot 10^{-4}$ Torr.

the role of a cross section for ion leakage from the beam region. If the ion lifetime τ_i in the beam region is much larger than the observation time t, then the derivative of the curves in Fig. 7 is approximately the same as the ionization cross section for nitrogen normalized to the beam protons. In the opposite case, the effective ionization cross section calculated in such a fashion (with no ion leakage taken into account) will be decreased, more substantially the smaller the value of τ_i/t is. The process of ion collection in the beam is analysed in considerable detail in the next section. Here attention is paid to the following two circumstances. First, the availability of the nearly horizontal part in the curves in Fig. 7 at the initial stage, prior to the development of instability, indicates that during this period the rate of ion production is approximately equal to that of ion leakage. The plasma density in the beam is proportional to the proton current. The effective "collection cross section" is close to zero. Second, after the beginning of the development of instability at gas pressures close to threshold and particularly in the above-threshold region, the rate of ion production increases dramatically. The effective ionization cross section calculated as a derivative of curve 3 in Fig. 7, *i.e.*, even without taking into account the loss of ions in the beam region as a result of their escape, reaches about $5 \cdot 10^{-16}$ cm^2 at an above-threshold pressure of nitrogen $3 \cdot 6 \cdot 10^{-4}$ during the development of the instability. This is three times higher than the cross section of nitrogen ionization by protons at an energy of 1 MeV, which is approximately $1.4 \cdot 10^{-16}$ cm^2. No faster ionization effect is observed when the gas pressure is much lower than the threshold (see curve 1 in Fig. 7). Similar results have been obtained in the experiments with the other gases.

All information about secondary-ion collection indicates that at the threshold gas pressure (and higher at the moment of development of the instability), the production of secondary ions occurs more rapidly as a result of ionization of the gas molecules by electrons.

Thus these observations allow the conclusion to be drawn that the condition for stabilization of the beam-beam instability of a cyclic compensated proton beam is the achievement of high density in the secondary plasma ($n_e \approx 3$ to $4 \cdot 19^8$). The threshold nature of the dependence of beam stability on gas density is explained by the fact that at threshold pressures the efficiency of ionization of gas molecules by secondary electrons sharply increases. It is noteworthy that the mechanism of effective ionization of a gas by secondary electrons begins working as soon as the instability occurs. It is likely to be a source of electron heating.

With further increase (over the threshold) in gas pressure, both the amplitude and the lifetime of the oscillations that are developed during collection reduce. The circulating proton beam, except a small (10 to 30 μsec) part in which the oscillations occur in the initial period of collection, becomes completely stable. However, the beam lifetime is greatly limited because of high gas density on the orbit.

At optimum gas pressures relative to the stored current, the measured lifetime of the protons introduced on the central orbit changed from 50 to 60 turns, depending on the gas being used to fill, in the absence of voltage at the accelerating gap (quasi-betatron mode). The comparison of the signals from the inserted targets has shown that the compression of proton orbits to the inner vacuum-chamber wall is a main source of losses in work with hydrogen and deuterium in the quasi-betatron mode. With an increase of the atomic number of the gas being used, enlargement of the transverse sizes of the beam begins playing a greater and greater role in limitation of the lifetime as a result of multiple scattering of protons on the molecules of the gas. So, in the work with argon in the above-threshold mode, a significant part of the beam loss was connected with an increase in its vertical dimension up to the aperture. The measured lifetime of the stable compensated proton beam is in good agreement with the calculated lifetime. The calculation takes into account the increase in beam dimensions because of multiple scattering of protons by gas molecules and also because of the orbit compression due to energy loss. The fact that the stored current is mainly limited by these two factors is additionally confirmed by the increase of the stored current when beam is placed in an outer orbit, especially in the work with light gases.

The beam potential measured over the energy spectrum of secondary ions was not higher than 10 to 30 V and was practically independent of the magnitude of stored proton current. The neutrality of the beam was also controlled by measuring the density of secondary ions and electrons in identical conditions. The total density of protons in the beam and secondary ions coincided, within good accuracy, with that of secondary electrons over a broad range of pressures (see Fig. 8).

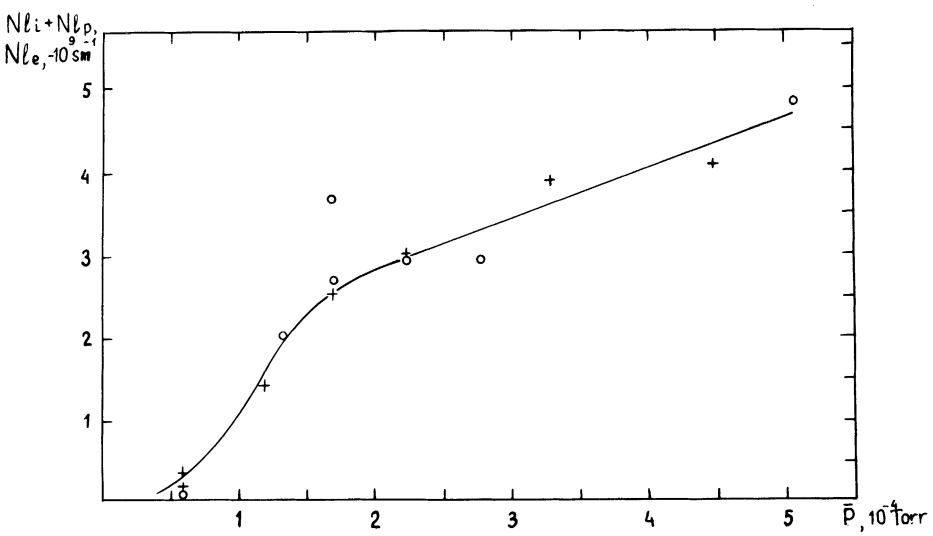

FIGURE 8 Total linear density of protons and secondary ions in the beam (+) and of secondary electrons (O).

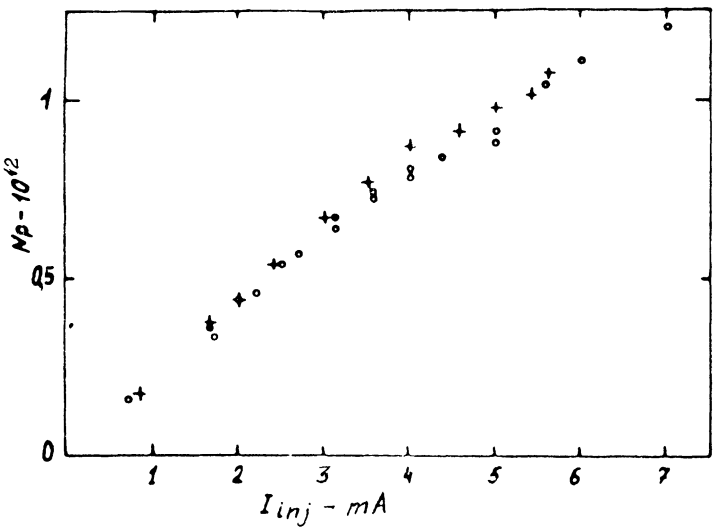

FIGURE 9 Number of stored protons as a function of injection current in the quasibetatron mode when filling with deuterium (+) and hydrogen (O).

Thus, since the time of current injection (up to 300 μsec) is much longer than the lifetime of a beam in the condition of stable compensation, the stored orbital current has to increase linearly with increasing injection current in the absence of limitations on its intensity; exactly this has been observed in the experiment (see Fig. 9). In the case of continuous pumping of the gas through the vacuum chambers of the storage ring, the number of protons stored under optimal pressures in the quasi-betatron mode is presented in Table IV.

As has already been mentioned, the lifetime of the beam and hence the current stored in the above threshold regimes of storage were completely determined by the gas density in the orbit. With a view to reducing the mean gas pressure that is necessary to store a maximum number of protons, we have made an attempt to vary the gas-density distribution over the azimuth by the pulsed leak-in system. In these conditions, a uniform distribution of gas pressure has proved to give optimal stored current. Such a system of gas leak-in has a positive influence on the increase of injection current in the above-threshold pressure region as a result of reducing the mean gas pressure in the transport line through which the beam has been transported from the injector. With constant pumping of the gas through the storage ring chamber (under pressures higher than the threshold one), the vacuum in the transport line was substantially degraded, which led to a decrease of the injected current because of the processes of stripping and scattering of the negative-ion beam on the gas molecules in the line.

TABLE IV.

Number of stored protons with various gases

Gas	H_2	D_2	He	N_2	Ar
N_p	$1.1 \cdot 10^{12}$	$1.25 \cdot 10^{12}$	$0.75 \cdot 10^{12}$	$1 \cdot 10^{12}$	$0.85 \cdot 10^{12}$

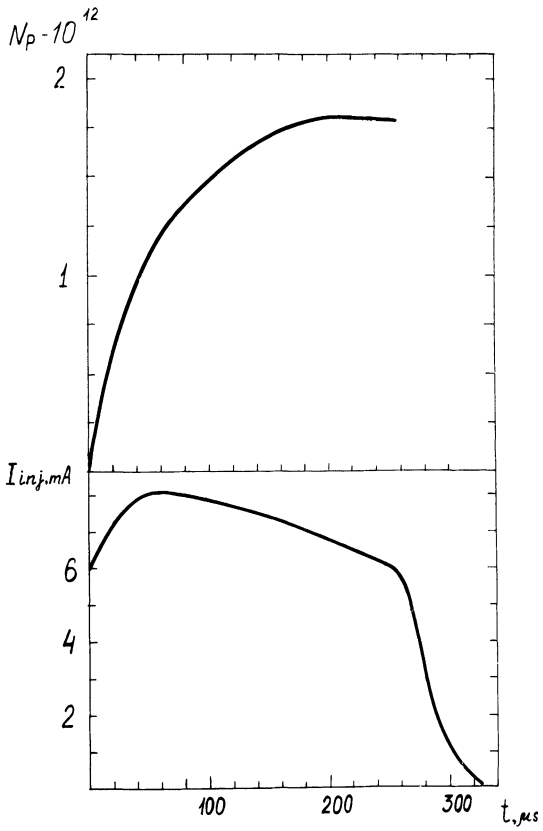

FIGURE 10 Oscillograms of stored protons in betatron mode (a) and the injection current (at the end of the first turn) (b) using pulsed pumping of hydrogen.

Switching on the acceleration voltage (betatron mode) enables the energy losses of protons to be partially compensated. Their lifetime on the orbit is 80 to 120. revolutions. Correspondingly, the stored proton current increases as well. The most noticeable increase in the number of the stored protons was observed in the work with hydrogen and deuterium. When the system was filled with argon, the compensation of energy losses had little influence on increasing the proton beam. This points to the fact that the role of multiple scattering in shortening the lifetime becomes more significant as the atomic number of gas grows.

In the betatron mode of storing, we have managed to store $1.8 \cdot 10^{12}$ protons using pulsed hydrogen pumping (see Fig. 10). This is 9.5 times higher than the limiting number of protons for a shift of vertical betatron-oscillation frequency up to the linear resonance, $\nu_z = 0.5$ and 6 times higher than for a shift of this frequency to zero.

3. FORMATION OF SECONDARY PLASMA IN THE BEAM REGION

When the beam of high-energy charged particle travels through the gas, the latter is ionized. Some plasma background arises in the beam region as a result. The electrons contained in this background plasma can, in turn, take part in the process of ionization

of the gas molecules, thereby increasing the rate of ion production. In most cases, the role of secondary electrons in plasma creation is negligible because the average energy of the electrons produced per act of ionization is low. (As has been shown in Refs. 21–25, the energy spectrum of electrons produced while ionizing the gas molecules by high-energy charged particles is such that their average energy lies in the region of the ionization potential for the initial molecules.) However, with the mechanism of electron heating available, gas ionization by the secondary electrons can become the major processes in the formation of plasma background.

The production of charged particles is accompanied by their escape from the beam region. It is the relation between the production and escape rate that determines the level of plasma density in the beam.

Let us write down a simple equation for the secondary-ion balance in the beam region

$$\frac{dn_i}{dt} = n_0 n_p \sigma_p v_p + n_0 n_e \langle \sigma_e v_e \rangle - \frac{n_i}{\tau_i}, \tag{1}$$

where n_i and n_e are the ion and electron densities in the background plasma, respectively, n_p is the proton density in the beam, σ_p, σ_e are the cross sections for ionization of the gas molecules by the protons and secondary electrons, respectively, v_p, v_e are the velocities of the protons and electrons, respectively, and τ_i is the lifetime of secondary ions in the beam region.

Let us take into account the quasineutrality condition: $n_i + n_p = n_e$. We obtain two solutions depending on the value of $n_0 \langle \sigma_e v_e \rangle \tau_i$. At $n_0 \langle \sigma_e v_e \rangle \tau_i \neq 1$,

$$\frac{n_i}{n_p} = \frac{n_{i0}}{n_p} e^{-(1 - n_0 \langle \sigma_e v_e \rangle \tau_i) t/\tau_i} + \frac{\sigma_p V_p + \langle \sigma_e V_e \rangle}{\frac{1}{n_0 \tau_i} - \langle \sigma_e V_e \rangle} [1 - e^{-(-n_0 \langle \sigma_e v_e \rangle \tau_i) t/\tau_i}]. \tag{2}$$

At $n_0 \langle \sigma_e v_e \rangle \tau_i = 1$

$$\frac{n_i}{n_p} = \frac{n_{i0}}{n_p} + n_0 (\sigma_p v_p + \langle \sigma_e v_e \rangle) t, \tag{3}$$

where n_{i0} is the ion density at $t = 0$.

Hence, at $n_0 \langle \sigma_e v_e \rangle \tau_i < 1$, *i.e.*, when the rate of ion leakage is higher than that of their production, it is possible for a steady state to occur. In this case, the density level in the secondary-ion beam is independent of the initial ion density and is determined by the relation

$$\frac{n_i}{n_p} = \frac{\sigma_p v_p + \langle \sigma_e v_e \rangle}{\frac{1}{n_0 \tau_i} - \langle \sigma_e v_e \rangle}. \tag{4}$$

Otherwise, continuous plasma collection occurs, which is linear at $n_0 \langle \sigma_e v_e \rangle \tau_i = 1$ and exponential at $n_0 \langle \sigma_e v_e \rangle \tau_i 1$.

As has already noted above, under pressures higher than the threshold, the secondary-plasma density in the beam region rapidly grows when the beam-beam instability is developed. Note that the measured rate of stacking of secondary ions is

much higher than that of ionization of the gas molecules by the beam protons. This points to the significant role of the plasma electrons in the formation of secondary plasma at that moment. It is natural to assume that a sharp increase in the rate of secondary-ion production at threshold gas pressures is associated with a transition to the plasma self-multiplication regime, when

$$n_0\langle\sigma_e v_e\rangle\tau_i \geq 1. \tag{5}$$

In our case, an analysis of this relation is complicated because there is no information about the velocity-distribution function of electrons and about the lifetime of secondary ions. Nevertheless, a number of the required evaluations may be done if one accepts the following assumptions.

(1) The energy-distribution function of electrons in a secondary plasma is independent of the kind of gas in the storage ring. This assumption is supported by the following factors. First, the distribution function of electrons produced in the course of ionization by charged particles depends in practice only on the potentials of ionization of the gas molecules, which coincide for all gases, except helium (24.5 eV) utilized in the experiment (15.4 to 15.7 eV).

Second, the plasma self-multiplication regime is realizable only during electron heating when the beam-beam instability arises, and the electron energy is likely to be mainly determined by the behavior of this instability, and the geometry of the proton beam and vacuum chamber.

(2) The lifetime τ_i of an ion in the beam, at a fixed average energy of electrons, is proportional to the square root of its mass and independent of the other parameters, *i.e.*, $\tau_i \sim \sqrt{m_i}$.

(3) The threshold pressure is determined by transition through a certain quantity, regardless the kind of a gas. This quantity is likely to be somewhat higher than unity.

Under these assumptions, the condition (5) can be written as

$$n_{0k}\langle\sigma_{ek} v_e\rangle\tau_{ik} = \chi_k(\bar{E}_e),$$

where k labels the kind of gas and $\bar{E}_e$ is the average electron energy; χ_k is a quantity of the order of unity, independent of the kind of gas. Then the quantity

$$\zeta_{k_1k_1}(\bar{E}_e) = \frac{\varkappa_{k_1}(\bar{E}_e)}{\varkappa_{k_2}(\bar{E}_e)} = \frac{n_{ok_1}\langle\sigma_{ek_1} v_e\rangle}{n_{0k_2}\langle\sigma_{ek_2} v_e\rangle}\left(\frac{m_{ik_1}}{m_{ik_2}}\right)^{1/2}$$

should become equal to unity at threshold pressures (see Table III). If one accepts a particular distribution function of electrons in velocity, one can determine their average energy from the condition $\zeta_{kk}(\bar{E}_e) = 1$. The dependences of $\zeta_{kk}(\bar{E}_e)$ for (a) monochromatic and (b) Maxwellian energy distributions of electrons are plotted in Fig. 11 (for various gases). The values of the cross sections and the rates of ionization of the gases by the electrons have been taken from Refs. 26 and 27. Hydrogen has been taken as a reference gas. It is seen that the condition $\zeta \simeq 1$ is satisfied for most of the gases studied at electron energies of 25–50 eV and is slightly dependent on the finite form of the distribution function. The strong difference observed for helium is probably connected with the initial distribution of electrons (with no heating taken into account), for it shifts to the high-energy side by 9 eV. That is, under otherwise identical

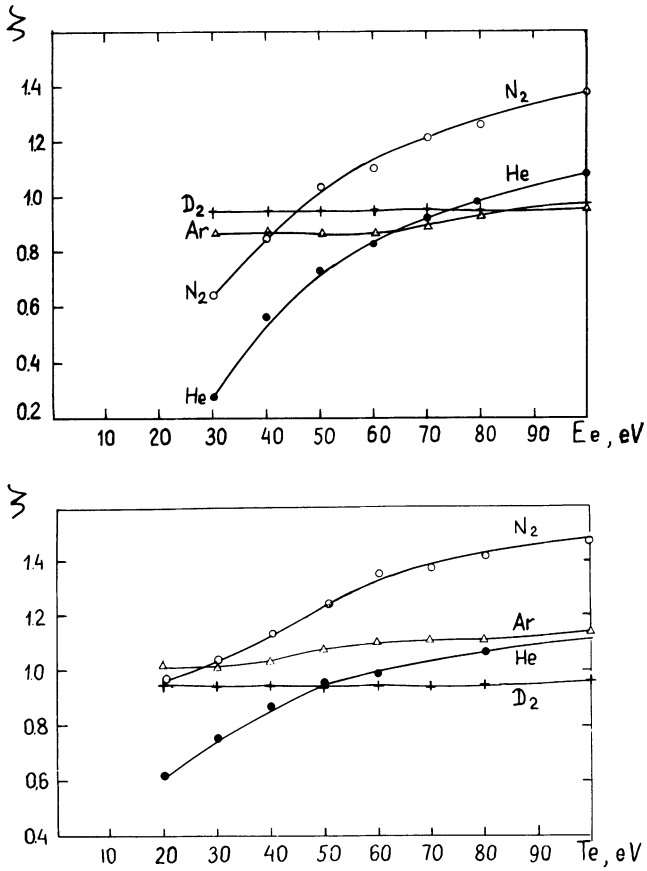

FIGURE 11 (a), (b)

conditions the average energy of electrons in a plasma is somewhat higher if helium is utilized than when other gases are used.

To calculate $\varkappa(\bar{E}_e)$, reasonable estimates of the lifetime of a secondary ion in the beam region need to be made. At a finite average energy of electrons in the nonequilibrium plasma ($T_e \gg T_i$, where T_e and T_i denote the electron and ion temperatures, respectively) the ions are extracted from the beam by the ambipolar potential and the average lifetime of ions τ_i is determined by the transverse half beam size a_z and by the ion-sound velocity v_i. Thus

$$\tau_i \approx \frac{a_z}{v_i} \approx a_z \sqrt{\frac{m_i}{T_e}} \tag{6}$$

The dependences of χ on the average energy of electrons calculated under these assumptions for the monochromatic (0) and Maxwell (+) distributions at the threshold pressure of hydrogen are shown in Fig. 12. It is seen that for $\bar{E}_e > 20$ eV in the case of the Maxwell distribution and for $\bar{E}_e > 30$ eV in the case of the monochromatic distribution the condition $\chi > 1$ is satisfied. The value of χ, which has been calculated without taking into account the electron heating, is also shown in this figure.* Here the

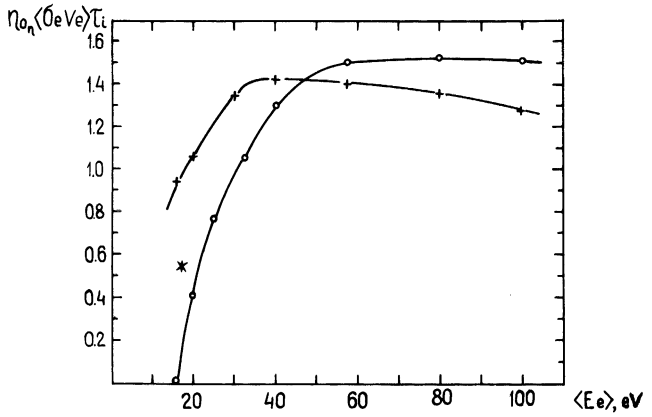

FIGURE 12

distribution functions of electrons produced in the process of ionization of the hydrogen molecules by the protons of the beam is taken as the velocity-distribution function of electrons.[22] In this case, $\chi < 1$ and the plasma self-multiplication regime does not occur. This is confirmed by experiment (see Figs. 5–7). Prior to the beginning of the development of instability, the plasma density is approximately proportional to the proton current.

Thus, the character of proton storage on an orbit prior to and after the threshold becomes clear. In the pre-threshold regime, the events develop as follows. In some interval of time after the beginning of injection, which is determined by the proton injection current and by the gas density on the track, an amount of electrons sufficient to develop the beam-beam instability is stored. Powerful coherent oscillations limit both the proton collection and the further increase of plasma density. After that, the plasma density is kept at some constant level determined by the rate of ion production and their lifetime [see Eq. (4)]. Although the electron energy is high enough, the gas density is insufficient to satisfy the condition (5).

When the threshold gas density is attained, prior to the appearance of the instability the situation remains qualitatively the same because the secondary electrons do not contribute substantially to the gas ionization, because of their low energy, and the proton current circulating on the orbit is still too small to ionize the gas up to the magnitude of plasma density necessary for stabilization. However, as the coherent oscillations develop, the situation becomes drastically different. Oscillations lead to fast heating of secondary electrons and these begin to ionize the gas effectively (see Fig. 7). The density of secondary ions rapidly increases, which results in the stabilization of the instability. Since the transition to the plasma self-multiplication regime is independent of the densities of the plasma and the proton beam from Eq. (5) and a significant contribution to the gas-ionization process comes from the secondary electrons, the threshold gas pressure should not be dependent on the magnitude of proton current. This independence has been observed in the experiment. The higher the gas density is, the faster the necessary plasma density is attained and the shorter the period of existence of the instability is.

After stacking a sufficient number of protons, electron heating by the instability cannot still be a necessary condition for obtaining a sufficient plasma density. Using Eq. (4), it is possible to find the proton density that is necessary to maintain the plasma density at a level of $4 \cdot 10^8$ cm^{-3} under a hydrogen pressure somewhat higher than the

threshold one; $n_0 = 1 \cdot 10^{14}$ cm^{-3} and in the absence of electron beating

$$n_p = n_i \frac{1/n_0\tau_i - \langle \sigma_e v_e \rangle}{\sigma_p v_p + \langle \sigma_e v_e \rangle} = 4.1 \cdot 10^7 \text{ cm}^{-3}.$$

Here τ_i is defined according to Eq. (6) at $T_e = 16$ eV. The calculated proton density corresponds to 130-mA current, which is consistent with experiment (see Fig. 4).

Note that the main contribution to gas ionization here is also given by the electrons, despite their low average energy. The rate of ionization of the gas molecules by the beam protons is given by the first term of the left-hand part of Eq. (1). At a current of 130 mA on the orbit ($n_p = 4.1 \cdot 10^7$ cm^{-3}), the protons form at the rate

$$\left.\frac{dn_i}{dt}\right|_p = n_0 n_p \sigma_p v_p \simeq 2.2 \cdot 10^{14} \text{ cm}^{-3} \text{ sec}^{-1}$$

per second. The contribution from the electrons is given by the second term of this formula

$$\left.\frac{dn_i}{dt}\right|_e = n_0(n_i + n_p)\langle \sigma_e v_e \rangle \approx 4 \cdot 10^{14} \text{ cm}^{-3} \text{ sec}^{-1}.$$

There is no difficulty in seeing that when storing high currents, the level of plasma concentration that is required to stabilize the instability ($n_i \approx 4 \cdot 10^8$ cm^{-3}) is achieved at lower and lower gas density in the absence of electron heating. The proton beam with maximum density, $n_p = 1.5 \cdot 10^8$ cm^{-3}, obtained in the experiments on hydrogen, is capable of providing the necessary level of plasma density with no electron heating at hydrogen pressure $\bar{P} = 1.5 \cdot 10^{-3}$. This is twice as small as the threshold one (see Table III). However, in this case it is necessary to suppress the instability that occurs during storing when the current is not yet high enough.

4. ANALYSIS OF THE CONDITIONS FOR STABILITY OF THE COMPENSATED PROTON BEAM

From the experiments, the density of secondary ions in the beam region is of the same order of magnitude or higher than the density of protons in the beam for practically the entire range of gas pressures. Therefore, in order to describe the beam motion, one needs take into account the interaction not only between the electron and proton beams, as is done in Ref. 11, but consider the interaction between the three distributions.[19,20]

Following the technique suggested in Ref. 11, we shall consider the interaction between cylindrical tubes of particles of the same radius, omitting the interaction between particles of the same kind. The density distribution of particles over the tube cross sections is assumed to be uniform. The proton beam has a directed velocity v_p in an azimuthal direction x. The secondary ions and electrons can freely travel towards in the vertical direction z and cannot move in other directions because of the guiding magnetic field. The orbit curvature in bending magnets is neglected. The forces of the beam-beam interaction may be regarded as purely transverse at sufficiently large wavelengths and small amplitudes of oscillations. The three tubes can move relative to

each other in the vertical direction and the polarization force per particle

$$\begin{aligned} f_p &= 2\pi e^2 n_e(z_e - z_p) - 2\pi e^2 n_i(z_i - z_p) \\ f_i &= 2\pi e^2 n_e(z_e - z_i) - 2\pi e^2 n_p(z_p - z_i) \\ f_e &= 2\pi e^2 n_p(z_p - z_e) + 2\pi e^2 n_i(z_i - z_e) \end{aligned} \tag{7}$$

acts between them, where f_p, f_i, f_e are the polarization forces acting on the protons, ions, and electrons, respectively, n_p, n_i, n_e are the densities of particles in the proton, ion and electron tubes respectively, and z_p, z_i, z_e are the transverse shifts of the corresponding tubes from the equilibrium position.

Moreover, the protons are subjected to the action of an external focusing force

$$f_z = -m_p \omega_z^2 z_p; \qquad \omega_z = V_z \omega_v, \tag{8}$$

where m_p is the proton mass, ω_z is the relative frequency of vertical betatron oscillations and ω_0 is the proton revolution frequency.

If the secondary particles are assumed to oscillate only vertically and their longitudinal velocity is assumed to be equal to zero, then the equations of motion will be of the form

$$\begin{aligned} \ddot{z}_p + \omega_z^2 z_p &= \frac{2\pi e^2}{m_p}[n_e z_e - n_i z_i - (n_e - n_i) z_p] \\ \ddot{z}_i &= \frac{2\pi e^2}{m_i}[n_e z_e - n_p z_p - (n_e - n_p) z_i] \\ \ddot{z}_e &= \frac{2\pi e^2}{m_e}[n_p z_p + n_i z_i - (n_i + n_p) z_e], \end{aligned}$$

where m_i and m_e are the secondary ion and electron masses, respectively. Here dots denote total time derivatives: $d/dt = \partial/\partial t + V\,\partial/\partial x$. The stability problem will be considered, as conventionally, in the linear approximation for perturbations of the form $z \sim \exp i(kx - \omega t)$ at $ka_z \ll 1$. Substitution into Eq. (8) gives a dispersion equation

$$F(w) = \frac{\omega_p^2}{(kV_p - \omega)^2 - \omega_z^2 - \omega_p^2 \delta / n_p} + \frac{\omega_e^2}{\omega^2 + \omega_e^2 \delta / n_e} + \frac{\omega_i^2}{\omega^2 - \omega_i^2 \delta / n_i} = 1, \tag{9}$$

where

$$\omega_e^2 = \frac{2\pi e^2 n_e}{m_e}; \quad \omega_p^2 = \frac{2\pi e^2 n_p}{m_p}; \quad \omega_i^2 = \frac{2\pi e^2 n_i}{m_i}$$

$$\delta = n_e - (n_i + n_p).$$

In the case of quasi-neutrality ($\delta = 0$), we obtain a dispersion equation similar to that investigated in Ref. 11

$$F(w) = \frac{\omega_p^2}{(kV_p - \omega)^2 - \omega_z^2} + \frac{\omega_e^2 + \omega_i^2}{\omega^2} = 1. \tag{10}$$

For the case

$$\frac{\omega_e^2 + \omega_i^2}{\omega_p^2} \approx \frac{\omega_e^2}{\omega_p^2} = \frac{n_e m_p}{n_p m_e} \gg 1$$

at

$$G = \frac{\omega_e}{\omega_z} \cdot \frac{n_p m_e}{n_e m_p} \ll 1, \tag{11}$$

the instability region lies, to good accuracy, in the band

$$kV_p = \omega_z + \omega_e(1 \pm G^{1/2}) \tag{12}$$

In the general case, the center of the instability band is determined by the sum of densities $n_i + n_p$ rather than by the electron density n_e. The major role of secondary electrons consists in shifting the instability band toward shorter wavelengths ($k \sim \omega_e \sim n_e^{1/2}$). The experimental value of the electron density, $n_e = 3$ to $4 \cdot 10^8$ cm^{-3} when the transverse rf oscillations stabilize corresponds to the length of unstable waves, $\lambda = 1.5$ to 2 cm. Transverse waves of such small length, comparable with the vertical size of the beam ($2a_z \approx 3.5$ cm) cannot apparently build up, although the increments of instability, at large enough wavelengths ($ka_z \ll 1$), increase with decreasing wavelength.[11] It follows from the experiments that the condition for stability of the proton beam in a plasma relative to transverse oscillations (which are connected with the beam-beam proton-electron instability) may be defined by

$$\lambda \lesssim a_z \qquad \text{or} \qquad n_e \gtrsim \frac{m_e V_p^2}{2\pi e^2 a_z^2}. \tag{13}$$

Thus, if a plasma of sufficient density is kept in the neighborhood of an orbit or one somehow achieves a high density in the electron-compensated beam, it is possible to attain many-fold values of the proton current in the accelerating ring over the space-charge limit.

We have not managed to explain, in terms of the linear approximation, the experimentally observed stability of the proton beam relative to the wavelengths that are comparable with its transverse dimension.[13] It seems very difficult to study the stability of the system at $ka_z \gtrsim 1$ when the wavelength is of the same order as the beam size and as the characteristic lengths of fall-off of the beam and plasma densities. Furthermore, the nonlinear phase of oscillations already starts at small amplitudes, and already this can lead to the instability becoming stabilized.

Some tendencies toward decreasing the increment at large magnitudes of k are observed in the linear approximation as well. For example, taking the finite wavelengths into account results in the polarization forces, acting on the particles being exponentially weakened to the beam center:

$$f \sim \frac{\cosh k_z z}{\cosh k a_z},$$

where z is the distance between the particle and the beam centre. For $ka_z < 1$, taking this effect into account causes a decrease of the increment by a factor $(1 + ka_z)$. The

stabilizing influence of the velocity spread of protons also becomes stronger as the value of k increases. And, finally, it is worth noting that with finite lifetime of the electrons, stabilization of the instability is achieved when the increment α is decreased to a small enough magnitude: $\alpha \lesssim 1/\tau_e$. In our case, τ_e lies within the limit $5 \cdot 10^{-7}$ to $2 \cdot 10^{-6}$ sec.

5. PLASMA GENERATION BY A FLUX OF ELECTRONS

As has been shown in Section 3, the condition for stabilization of the beam-beam instability of the compensated proton beam is the availability of a plasma of 3 to $4 \cdot 10^8$ cm^{-3} density within the beam region. Because of the low efficiency of residual gas ionization by the circulating protons, the necessary plasma density is achieved only at sufficiently high gas pressure in the storage ring. The lifetime of the intense stable compensated beam of protons is strongly restricted under these conditions. Plasma generation due to the ionization of gas molecules by the protons cannot therefore be used, as a rule, for suppression of the beam-beam instability in accelerators. Other methods of plasma generation are required in accelerators.

For plasma generation in the storage ring, we have chosen the ionization of residual gas by the flux of electrons travelling along a magnetic field and perpendicularly to the proton beam. A rectilinear multiwire thermocathode spaced above or below the proton beam has been employed as a source of electrons. In practice, the feasibility of such a method is largely dependent on how effective the utilization of electrons is. For plasma generation, the optimum range of energies lies between 50 eV and 150 eV. However, obtaining electron currents of such an energy with wire thermocathodes is rather complicated because of the requirements for small gaps in the extraction system. In view of this, in the scheme chosen for an ionizer, the primary beam of electrons with relatively high energies is converted, after it has crossed the aperture of the storage ring, to a backward flux of electrons with energy of about 100 eV. A cold flat plate with coefficient of secondary electron emission $\kappa > 1$ in combination with a fine-cell extraction grid placed close to its surface is used as a converter. For most metals, the coefficient of secondary electron emission has a broad maximum in the energy range of primary electrons (400–1000 eV); therefore, the extraction voltage for primary electrons can be high enough. The possibility, in principle, of a many-fold increase of the flux of electrons in the operating region by use of special materials with $\kappa \sim 10$ substantially eases the requirements on the thermocathode and extraction system of primary electrons.

Following from the arguments listed above, the layout schematically shown in Fig. 13 has been taken as a reference. The residual gas ionizer consists of two parts, cathode and converter units placed above and below the proton beam. The thermocathode is a few thin wires stretched along an orbit of the proton beam. The distance between the wires is dictated mainly by the requirements for plasma homogeneity in the proton beam region. Below each wire of the cathode and parallel to it, there are two threads of a primary extraction grid (2) with a 2-mm-wide extraction slit formed by these threads. Since the thermocathode wires are located between the extracting threads and are much thinner than the extraction slit, the extraction gap is magnetically isolated and a transverse electric field is generated for impact broadening of the electron flux across the magnetic field. The fact that electrons acquire transverse velocities in localized electric fields is also useful to attenuate non-isotropic instability in the plasma being produced.

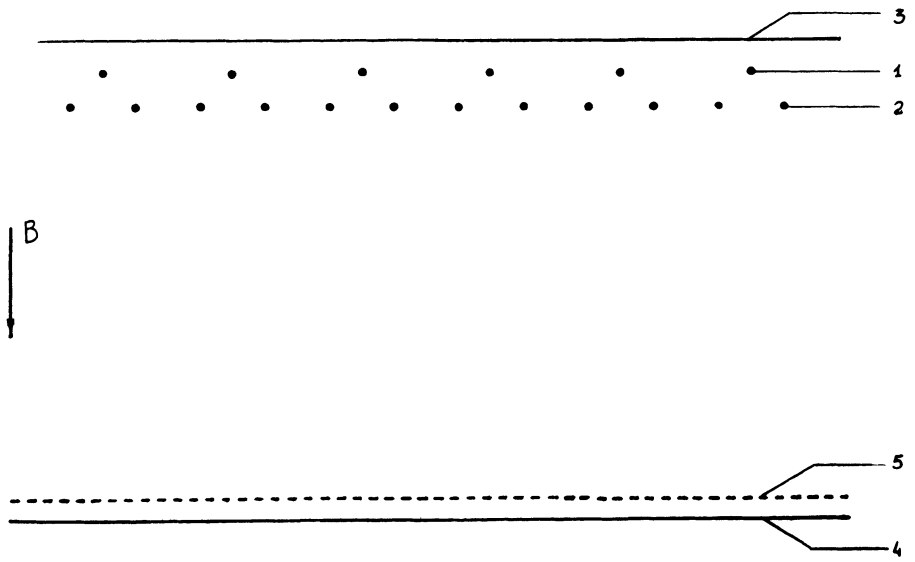

FIGURE 13 Layout of the residual gas ionizer: 1—thermocathode wire, 2—extraction grid, 3—reflecting plate, 4—secondary-emission plate of the converter, 5—converter grid.

The primary and secondary extracting (negative) potentials are supplied to the cathode and to the secondary-emission plate of the converter, respectively. The cathode and converter grid are grounded.

In order to extract electron current of high enough density, at a converter potential of about 100 V, it is necessary that the gap between the secondary-emission plate of the converter (4) and its grid (5) be sufficiently small. The simple geometry and the absence of thermal deformations lead to this requirement becoming relatively easy to meet. Using available materials, we have fabricated a residual-gas ionizer that is specially intended for experiments with our storage ring at a magnetic field in the bending magnets of 3.5 kG. The cathode is made from thoriated tungsten with an emission capability of 3 A/cm^2 at about 1800°C operating temperature. The cathode wires are 0.19 mm in diameter spaced by 7 mm. The primary extraction grid is fabricated from Ni-Cr alloy wire 0.2 mm in diam. Because the oil pumping used in the storage ring does not give the possibility for work with effective emitters of secondary electrons, we have chosen copper with $\kappa = 1.3$ as a material for the converter plate. The converter grid is woven from tungsten 30 mcm-diam wire with 150 mcm × 150 mcm square mesh. Its transparency is 70%. The extraction gap in the converter is 0.7 mm.

For the emission current to be completely extracted according to the "3/2 law", the cathode must be fed by a voltage of about 900 V. In this case, the mean density of primary electrons will be 0.13 A/cm^2. The presence of the transverse electric and space-charge fields in the extraction region leads to the flux of electrons from the thermocathode wire becoming much enlarged. The calculated maximum density of secondary electrons will amount to about 0.7 A/cm^2. In order to extract electrons of such density through the 0.7 mm gap, a voltage of 120 V is used. The mean density of secondary electrons from the converter will be about 0.12 A/cm^2. With the chosen geometry of the cathode part of the ionizer, the secondary electrons from the converter are reflected without loss in the electric field of cathode and traverse twice the aperture. With this taken into account, the ionizer should generate, in the operating region, two

groups of electrons with mean densities $\bar{n}_1 \approx 4.5 \cdot 10^8$ cm^{-3} and $\bar{n}_2 \approx 2.6 \cdot 10^9$ cm^{-3} at energies of 900 eV and 120 eV, respectively. As a result, the chosen scheme of plasma generation makes it possible to create a plasma of density $\bar{n} \geq \bar{n}_1 + \bar{n}_2 \approx 3 \cdot 10^9$ cm^{-3} on the accelerating orbit in the electron charge-compensation period of approximately 10^{-5} sec under a residual-gas pressure of 10^{-5} Torr.

Experimental study of the performance of ionizers in the course of experiments has shown that they allow the production of a calm plasma with a density of 10^9 cm^{-3} and higher.[28] Note that the plasma inhomogeneity (on account of the cathode discreteness) was relatively small (the plasma band width from each, separately was switched-on, wire of the cathode was about 1 cm in size).

The design of the storage-ring vacuum chamber did not enable one to work at a constant filament voltage of thermocathodes because a great number of elements are made from heat-unstable materials. In this connection, the cathodes were heated by powerful current pulses of about 100 msec in duration directly prior to the runs. The pulsed filament supply of thoriated-tungsten cathodes resulted in a fairly substantial increase of gas pressure in the storage-ring chamber because of the volumetric absorption of the residual gas between pulses and also because of the gas desorption from the components of the ionizers and the vacuum chamber under the action of light and the electrons of a gas stored on the surfaces between the pulses.[28] For example, the mean gas pressure in the storage ring increased to $\sim 2.5 \cdot 10^{-4}$ Torr because of these effects while achieving a mean plasma density in the ionizers of $\sim 10^9$ cm^{-3}.

However, the gas desorption from ionizers in no way precludes their application to stabilize the beam-beam instability in ring accelerators. With the use of high-temperature suspension insulators for thermocathodes and in the absence in vacuum chambers of heat-sensitive materials, the ionizers can operate in the constant filament-supply regime. Experiments have shown that in this case the gas desorption from ionizers can be decreased nearly by two orders of magnitude even with no special measures to reduce gas desorption from the surfaces irradiated by the electrons.[28]

It seems promising to use the thermocathodes made from lanthanide-content Ir in ionizers; this makes it possible to reduce their operating temperature. Oilless pumping in the accelerators enables plate materials with high coefficient of secondary electron emission, $\kappa \sim 10$, to be used as secondary-emission converters. These will permit a substantial improvement of the ionizer parameters.

The chambers in all bending magnets as well as the first and second straight sections have been equipped with two ionizers each. Two ionizers of half-width have been mounted in the third section. In total, the storage ring has been equipped with 14 ionizers; the total operating length of these ionizers is equal to half the length of the storage ring orbit. In order to reduce the influence of electric fields in ionizers on the proton beam, the cathode and converter parts have been interchanged in each subsequent ionizer. Since the ionizers are in a magnetic field, the ultrasonic generators USG2-4, specially fabricated for operation in the pulsed mode, have been used as the sources of filament current for the cathodes. The emission currents of the thermocathodes have been adjusted by varying the duration of the filament pulse.

6. EXPERIMENTS ON STABILIZATION OF THE COMPENSATED PROTON BEAM WITH IONIZERS

Proton-beam storage as a function of the density of a plasma generated by ionizers has been studied as follows. By controlling the duration of the filament pulses, the

thermocathodes were heated up to approximately the same temperature so that the linear density of emission current was equal in all the ionizers. The thermocathodes were supplied in such a way that the heat pulses were completed simultaneously in all ionizers. The extraction voltage was supplied to the ionizers' cathodes for several microseconds after the heating of the cathodes had been completed. The amplitude of the extraction voltage was the same in all the ionizers. The extraction pulses were supplied synchronously to all the ionizers. The duration of the extraction pulses and their position relative to the injection pulses of protons could be varied in a broad range. The secondary-emission plates of converters were at a constant potential of -120 V.

The action of sagging electric fields in the ionizers on the behavior of protons was measured directly on the beam. To do this, voltage was supplied to the cold cathodes and to the secondary-emission plates of the converter during proton collection at different gas pressures. At the limiting vacuum, $\bar{p} \approx 1 \cdot 10^{-5}$ Torr, and with the extraction voltage switched on, the amplitudes of rf signals from the vertical beam-position pick-ups and from the quadrupole-signal electrodes were somewhat decreased. This effect became less significant with increasing gas density and at $\bar{p} = 7 \cdot 10^{-5}$ Torr and higher, the action of the extraction voltage on the storage of proton beam was not observed. No shift of betatron frequencies was seen during the switching on the extraction voltage.

At first, we have studied the storage of proton beam as a function of plasma density in the ionizers with continuous plasma generation by the ionizers during the existence of the beam on the orbit. The behavior of the proton beam versus the emission current of the ionizers, to which the density of the plasma generated by them is approximately proportional, is illustrated in Fig. 14. On account of the gas desorption of thermocathodes when they were heated in a pulsed manner to a temperature corresponding to the appearance of a noticeable emission current, the minimum mean gas pressure on the orbit was equal to $1 \cdot 10^{-4}$ Torr. In the absence of emission current of electrons from the cathodes (because of their low temperature), the plasma on the orbit is produced by ionizing of gas molecules by the protons of the beam and by secondary electrons. Since the gas pressure on the orbit is lower than the threshold that is necessary to transit to the plasma self-multiplication regime and since its density is insufficient to stabilize the beam-beam instability, intense rf oscillations develop in the beam. With an increase of emission current from the cathodes, the electron fluxes in ionizers play a greater and greater role in plasma generation. The mean plasma density on the storage ring orbit increases. At first, this increases the instability and, correspondingly, the orbital protons current falls off. The minimum stored current corresponds to a mean plasma density in the ionizers of about $1 \cdot 10^8$ cm^{-3}. The amplitude of oscillations gradually decreases as further increase of the emission current occurs. The stored current of protons grows. The maximum of the spectrum of proton-beam oscillations shifts toward short wavelengths. However, an increase of the emission current is accompanied by an increase of the gas pressure on the orbit due to gas desorption from the surfaces irradiated by electrons. This shortens the lifetime of protons on the orbit and limits the number of stored protons.

Comparative measurements have been made on the lifetime of protons in a low-intensity beam in which the instability does not develop. During these measurements, the mean gas density was approximately equal, but in one case it was due to the performance of the ionizers and in the other case due to a filling of nitrogen. The influence of plasma generation on the lifetime of protons has not been seen within the accuracy of our measurements. The lifetime of protons in the storage ring was determined by gas density on the orbit.

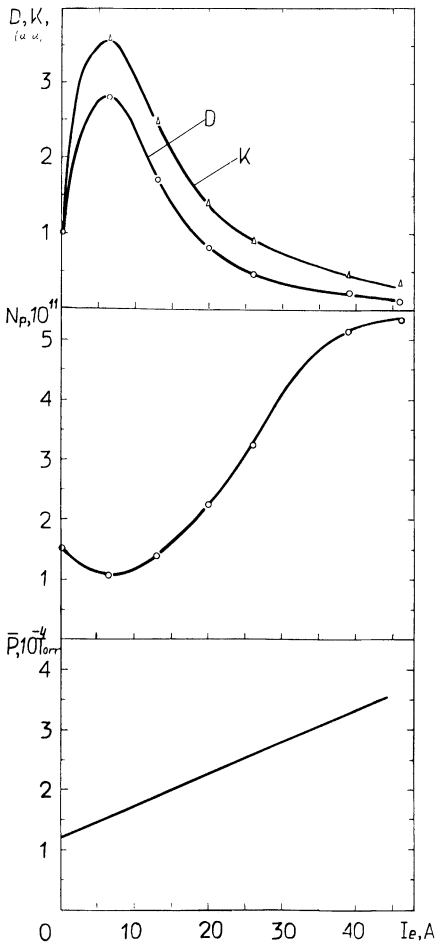

FIGURE 14 Dependencies on the emission current in the ionizers: $\bar{P}$ is the mean gas pressure on the orbit; N_p is the maximum number of protons in the beam; D is the amplitude of rf signals from electrostatic electrodes of vertical position of the beam per unit orbital proton current; K is the same for quadrupole electrodes.

From the qualitative point of view, the behavior of a proton beam as a function of the density of a plasma generated by ionizers (Fig. 14) is similar to its behavior in the ionized gas on the track with no outer ionizers (see Fig. 3). At low plasma density, its growth causes the instability to increase and the stored proton current falls off. At a plasma density higher than 3 to $5 \cdot 10^8$ cm^{-3}, the beam-beam instability stabilizes and the stored current is mainly limited by the multiple scattering of protons by the gas molecules on the track.

There are, however, substantial discrepancies. In the case of plasma production by a proton beam and secondary electrons, there is a clear gas-density threshold in a storage ring. This threshold is associated with the fact that in the transition through the threshold gas pressure, the plasma density increases stepwise as a result of the effective ionization of the gas molecules by electrons with provision for satisfying the condition (5). The parameters of the proton beam, together with the density of a background

plasma, are varied dramatically. This is because a sharp increase of the plasma density in the beam gives rise to a corresponding shift of the instability band toward short wavelength (12), where the instability stabilizes.

If the plasma is generated by ionizers, the plasma density in the beam is a controllable quantity. Its smooth change leads, as is seen in Fig. 14, to gradual damping of the instability that is associated with a smooth shift of the instability band to the side of short wavelengths.

Thus, the observed regularities in the behavior of a proton beam when varying the emission current in ionizers, *i.e.*, the absence of a clear threshold in the stabilization of the instability, confirm that it is the plasma generated by ionizers that plays a dominant role in stabilization of the beam-beam instability. Moreover, the oscillations of the proton beam start stabilizing under a gas pressure on the track which is 2 to 3 times less than the threshold one, equal to $3.2 \cdot 10^{-4}$ Torr, for nitrogen.

The oscillograms in Figs. 15 and 16 clearly demonstrate the influence of the plasma from ionizers on the stability of a proton beam. These show the behavior of the proton beam when the extraction voltage on the cathodes of the ionizers is switched on (a) and it is switched off (b) rapidly during the proton-beam storage. In the first case, the plasma density begins increasing rapidly due to the ionization of gas molecules by the flux of electrons from cathodes and converters. However, the gas density also increases when the emission current appears. In the second case, only one external parameter varies in

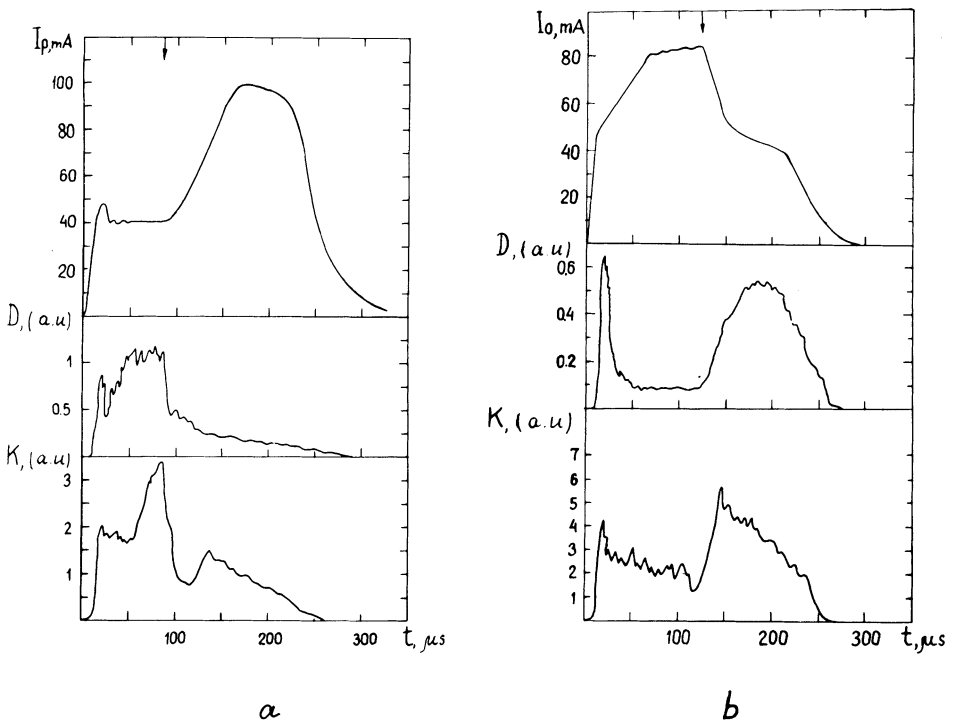

FIGURE 15 Proton current I_p and the envelopes of rf signals from the electrostatic vertical-position electrodes (D) and from the quadrupole oscillations transducer (K) of a proton beam. (Copies of oscillograms). The emission current in the ionizers is 25 A. The arrows indicate the times of switching on (a) and switching off (b) the extracting voltage.

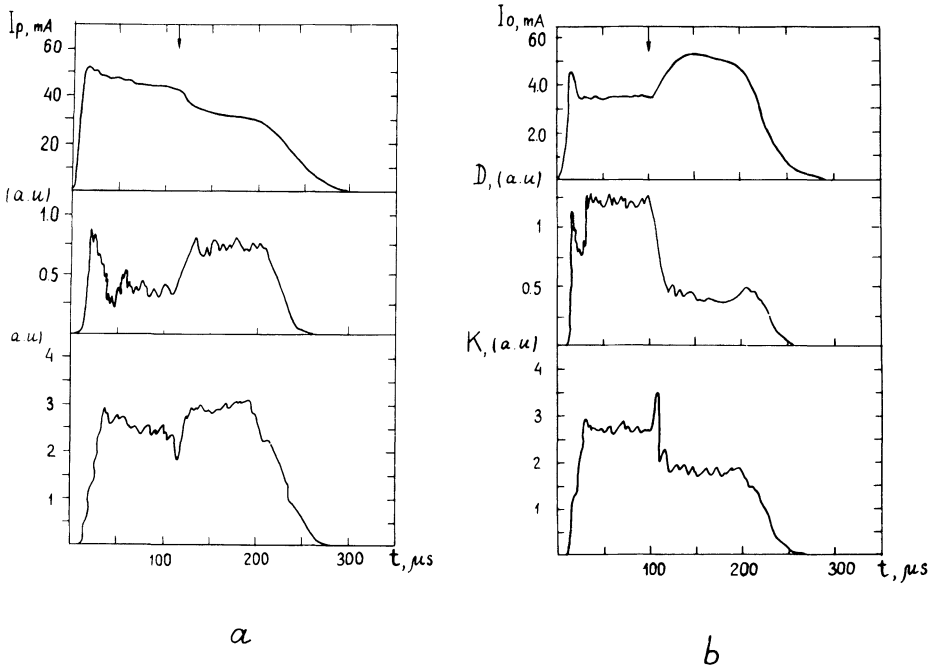

FIGURE 16 The proton current I_p and the envelopes of rf signals from the electrostatic vertical-position electrodes (D) and from the quadrupole oscillations transducer (K) of a proton beam. (Copies of oscillograms). The emission current in the ionizers is 6.5 A. The arrows indicate the times of switching on (a) and switching off (b) the extracting voltage.

the course of proton collection: the plasma density reduces rapidly (the decay time of a plasma generated by ionizers amounts, as the experiments have shown[28], to several microseconds). With the ionizers switched off, the gas density in the storage ring does not vary during the end of beam stacking.

After switching on the extraction voltage in the ionizers, a plasma of sufficient density, $n_e \geq 5 \cdot 10^8$ cm^{-1}, is generated, the amplitude of proton oscillations reduces drastically, and the stored current of protons becomes much higher (see Fig. 15a).

Switching off the extraction voltage, which is accompanied by an appreciable decrease in the plasma density in the ionizers, leads to a rapid development of the instability and to a sharp decrease of the proton current (Fig. 15b). The behavior of the beam when switching off the extraction voltage on the ionizers unambiguously indicates that the gas density on the track is not sufficient to create the conditions necessary for stabilizing the instability with no additional plasma generation.

The availability of a certain level of beam oscillations when the ionizers are switched on may be accounted for by the fact that the plasma generation has occurred only on half the length of the proton orbit. We have observed a similar effect in case of the non-uniform (over azimuth) distribution of gas density on the track during our stabilization experiments without ionizers.

The increase in the plasma density when the extraction voltage is switched on and the emission current is low, causes the growth of the instability (see Fig. 16a, b). It is quite consistent with the behavior of the instability at a low plasma density when sufficiently long wave oscillations develop.

In the experiments on stabilization of the beam-beam instability of a compensated proton beam by a plasma generated by ionizers, we have failed to exceed the maximum amounts of the stored proton currents obtained by us earlier. This can be understood as follows. The vertical aperture of the vacuum chambers in the bending magnets was somewhat decreased when installing the ionizers. For technical reasons, we had no possibility of adjusting the storage ring after the installation of these ionizers. The focusing properties of the storage ring magnetic orbit were changed as a result. As a consequence of the degradation of the accelerating tube in the injector, the quality of the injected beam worsened. The layout of the storage ring permitted less than half the length of the storage ring to be provided with ionizers, which resulted in the existence of a high enough level of oscillations of the beam at sufficiently high concentration of the plasma in the ionizers.

During the optimum mode of operation of the ionizers, $5.3 \cdot 10^{11}$ protons was stored. With the decreased aperture of the vacuum chambers in the storage ring, this figure is three times higher than the space-charge limit. Under similar conditions, with the ionizers off during the filling of the gas, the maximum number of stored protons did not exceed, for the reasons cited above, approximately $3.8 \cdot 10^{11}$.

Thus, the results obtained are evidence for the validity of our interpretation of the stabilization mechanism of an instability and enable one to hope that this method will offer the possibility of eliminating the space-charge limit in the process of proton-beam stacking in accelerators at an acceptable gas density on the orbit by means of measures to reduce gas desorption from the ionizers and to provide a larger fraction of the accelerating track with a plasma.

After the storage of a compensated proton beam of sufficient intensity, $n_p \geq m_e V_p^2 / 2\pi e^2 a_z^2$, there is no necessity for external plasma generation.

The possibility cannot be ruled out that the intensity of the compensated proton beam in the accelerating ring can be increased by the order of 10^3 times compared to the space-charge limit and its magnitude will be restricted by short-wave longitudinal instabilities at the plasma frequency of protons.

7. ACKNOWLEDGEMENTS

The authors are indebted to V. G. Shamovsky and V. G. Roslyakov for joint work and helpful discussions and to V. S. Belkin for development of radio engineering devices.

REFERENCES

1. G. I. Budker and G. I. Dimov, International Conf. on Accelerators, Dubna, 1963, Moscow, 933 (1964).
2. G. I. Budker, G. I. Dimov, A. G. Popov, Yu. K. Sviridov, B. N. Sukhina, and I. Ya. Timoshin. *At Energ.* **19,** 507 (1965).
3. Proc. of the 5th Intern. Conf. on High Energy Accelerators, Frascati 1965, 399 Roma (1966).
4. G. I. Budker, G. I. Dimov, and V. G. Dudnikov, Proc. of the Intern. Symposium on Storage Rings. Sacley, France VIII-6-1 (1966).
5. G. I. Budker, Proc. of the 5th Intern. Conf. on High Energy Accelerators, Frascati, 1965, Roma, 402 (1966).
6. N. Christofilos, USA Patent No 2894456 (p. I. 150–27), 1953.
7. G. I. Dimov, V. G. Dudnikov, and V. G. Shamovsky, *At Energy.* **29,** 356 (1970).
8. A. A. Kolomensky and A. N. Lebedev, *At. Energ.* **7,** 549 (1959).
9. G. I. Dimov, V. G. Dudnikov, A. A. Sokolov, and V. G. Shamovsky, *At. Energ.* **27,** 130 (1969).
10. G. I. Budker, *At. Energ.* **1,** 9 (1956).
11. B. V. Chirikov, *At. Energ.* **19,** 239 (1965).

12. O. Koshkarev and P. Zenkevich, *Particle Accelerators* **3,** 19 (1972).
13. G. I. Dimov, V. G. Shamovsky, and V. E. Chupriyanov, Proc. of the 2nd National Meeting on Charged Particle Accelerators. Moscow, 1970 (*Moscow*, "*Nauka*", **2,** 20, 1972).
14. G. I. Dimov, V. G. Shamovsky, and V. E. Chupriyanov, *J. Theor. Phys.* **41,** 2098 (1971).
15. G. I. Dimov, V. G. Shamovsky, and V. E. Chupriyanov, Proc. of the 3rd National Meeting on Charged Particle Accelerators, Moscow, 1972 (*Moscow*, "*Nauka*", **vol. 1,** 349, 1973).
16. K. Hübner, E. Keil, and B. Zotter, CERN-ISR-TH/71-46.
17. H. Grunder and G. Lamberston, Proc. of the 8th Int. Conf. on High Energy Accelerators, CERN, Geneva, 1971, p. 308.
18. E. Keil, Interacting Storage Rings, Rep. No CERN, Geneva, 1972.
19. G. I. Budker, G. I. Dimov, G. V. Roslyakov, V. E. Chupriyanov, and V. G. Shamovsky, Preprint INP 77–51, Novosibirks (1977).
20. Yu. I. Bel'chenko, G. I. Budker, G. E. Derevyankin, G. I. Dimov, V. G. Dudnikov, G. V. Roslyakov, V. E. Chupriyanov, and V. G. Shamovsky, Proc. of 10th Intern. Conf. on High-Energy Charged Particle Accelerators, Protvino, 1977, *Serpukhov*, **1,** 287 (1977).
21. D. R. Bates and G. Griffing, Proc. of the *Phys. Sec. A* **66,** part II, 961 (1953).
22. M. Grisinski, *Phys. Rev.* **138,**322 (1965).
23. C. E. Kuyatt, and Th. Jorgensen, *Phys. Rev.* **130,** 1444 (1963).
24. M. E. Rudd, and Th. Jorgensen, *Phys. Rev.* **131,** 666 (1963).
25. M. E. Rudd, C. A. Saatter, and C. L. Bailey, *Phys. Rev.* **151,** 20 (1966).
26. N. I. Alinovsky, Yu. E. Nesterikhin, and B. K. Pakhtusov, *J. Theor. Phys.* **39,** 139 (1969).
27. C. F. Barnett et al., Atomic Data for Controlled Fusion Research ORNL-5206, 1977.
28. V. E. Chupriyanov, Preprint INP 80-154, Novosibirsk (1980).